OST ANNUAL TECHNICAL PROGRESS REPORT – FY2001
Reciprocating Engines Team

Team Members: Michael H. McMillian, Phouc Tran, Steve Richardson, Steve Woodruff, John Ontko and Fred White

DESCRIPTION: During Fiscal Year 2001, the Reciprocating Engine Team worked in the following areas:

- Mutagenic (health effects) effects of particulate matter from both standard diesel fuel and Fischer-Tropsch-derived fuel in diesel engines.
- Engine emissions and combustion performance of Fischer-Tropsch-derived fuel in a diesel engine.
- Modeling of natural gas engine knock phenomena.
- Laser ignition of natural gas with applications to reciprocating engines.
- Development of a large-bore rapid compression machine for fundamental in-cylinder combustion studies.

RESEARCH OBJECTIVES:

Fischer-Tropsch-derived engine fuels:

- Perform combustion, engine performance, and emissions analysis of Fischer-Tropsch-derived fuels.
- Conduct bioassay analyses to determine mutagenicity of particulate matter from Fischer-Tropsch-derived fuels.

Natural gas engine knock abatement:

- Develop a novel rapid compression constant volume combustion apparatus (RCM) for studies of natural gas engine combustion knocking mechanisms and development of knock mitigation strategies.
- Develop a commercial CFD-based natural gas engine knock model in collaboration with Fluent Inc.

Laser ignition studies:

- Conduct studies on the physics and chemistry of laser ignition.
- Develop a database and theoretical models for predicting and evaluating spark generation, spark absorption, concentrations of exited species, temperature, pressure, dynamic evolution of a laser spark, and the laser ignition process.

LONG TERM GOALS:

Continue engine combustion developmental support for liquid transportation fuels. Develop engine knock control strategy using novel geometries and laser ignition. Develop a durable ignition source for high BMEP natural gas-fueled engines using a laser as an ignition source.

RESULTS: This section is divided into three parts corresponding to research projects in (1) ultra-clean liquid fuels, (2) knock in natural gas engines, and (3) laser ignition studies.

1.0 Combustion and Emissions Performance With Fischer-Tropsch Liquid Transportation Fuels

Description:

Growth of diesel engines in the light-duty and heavy-duty vehicular market has continued to focus attention on the health risks of diesel exhaust. From a regulatory perspective, particulate matter in diesel engine exhaust is becoming less tolerable. The California Air Resources Board and the Office of Environmental Health Hazard Assessment has identified diesel exhaust as a toxic air contaminant. The International Agency for Research on Cancer concluded that diesel particulate is a probable human carcinogen (IARC, 1989). Cleaner burning liquid fuels, such as those derived from natural gas via the Fischer-Tropsch (FT) process, offer a potential economically viable alternative to standard diesel fuel while providing reduced particulate emissions. Further understanding of

FT operation may be realized by investigating the differences in potential health effects between particulate matter derived from FT fuel and that derived from standard federal diesel No. 2 (DF). This project examines the mutagenicity of particulate matter derived from FT and DF fuel combustion in a single-cylinder diesel engine. This is done using the Ames Salmonella test to relate the in-vitro mutagenic activity of the particulate to engine operating conditions and particle size. Total particulate matter (TPM) samples are gathered using glass fiber filters in a mini-dilution tunnel from engine operation on each fuel at seven steady-state engine operating conditions. Particulate matter from two engine conditions are also gathered on greased aluminum foil substrates using a micro-orifice uniform deposition impactor (MOUDI) for size selective mutagenic analysis. Toxicity effects are reported but screened from the dose-response analysis using a method similar to that set forth by Bernstein et al (1982). Results indicate mutagenic response differences in the particulate matter as functions of engine operating conditions, fuel type, and particle size, with larger particles exhibiting a significantly greater mutagenic effect than their smaller counterparts.

The emissions reduction of Fischer-Tropsch (FT) diesel fuel has been demonstrated in several recent publications in both laboratory engine testing and in-use vehicle testing. Reduced emission levels have been attributed to several chemical and physical characteristics of the FT fuels, including reduced density, ultra-low sulfur levels, low aromatic content, and high cetane rating. Some of the effects of these attributes on the combustion characteristics in diesel engines have only recently been documented. As part of this study, a Ricardo Proteous, single-cylinder, 4-stroke DI engine was instrumented for in-cylinder pressure measurements. The engine was run at several-steady engine states at multiple timing conditions using both federal low sulfur diesel fuel and a natural gas-derived FT fuel. The emissions and performance data for each fuel at each steady state operating condition were compared. The cylinder pressure data were used to determine a suite of thermodynamic indicators, which are used to help explain the emissions variations between fuel types.

Accomplishments: Specific conclusions from this work are as follows:

- When considering cases other than low-load conditions, the relative reduction in TPM from FT fuel was 26% over the DF fuel.
- When coupled with TPM production rate, the FT fuel provides a 45% reduction in revertant rate (rev/hr) (a measure of mutagnicity) over the DF fuel averaged over key states 3, 4, 7 and 8 and 38% over all operating conditions (key states).
- Size fractionated MOUDI DPM Ames analysis was performed with 2 bacterial strains both with and without S9 activation for 2 size groups. The small-size group (2 sm and 4 sm) was made up of substrates 9, 10, and the afterfilter and represents the “ultra-fine particles” or particles with nominal diameters less than 100 nm (0.1 μm). The second grouping (2 lg and 4 lg) consists of substrates 3-8 and represents particles with nominal diameters between 100 nm (0.1 μm) and 3.1 μm.
- The analysis of variance on the MOUDI samples is based on 2 levels of fuel type (DF and FT), 2 levels each of Salmonella strain and S9 activation, 2 size fractions, and 2 operating conditions (key states).
- Significant differences in mutagenicity between fuel type, key state, and particle size is indicated.
- Second and third order interactions between fuel, key state, and particle size are indicated in the dose response.
- Larger particles tend to exhibit a significantly larger mutagenic response than smaller size particles. This has implications with regard to emissions control, as larger particles tend to be more efficiently removed in diesel particulate traps. The remaining smaller particles may very well exhibit reduced mutagenicity in regards to their SOF content.

The following conclusions may be drawn from testing using the Ricardo Proteous, single-cylinder, 4-stroke DI engine in this study:

- In general, each operating condition displays similar trends for each of the two test fuels, implying that while the absolute emissions levels are different their trends are similar with respect to changing engine conditions.
- Any relationship between NO_x and location of the diffusion peak appears to be a covariant relationship with timing. Further, there is no functional relationship between NO_x and differences of location of the maximum diffusion heat release rate.
- NO_x did not appear to be a significant function of exhaust temperature for any key state.
- The diffusion peak of the heat release rate was consistently greater for FT fuel, while the location of the diffusion peak was covariant with the location of the start of combustion as well as the 50% to 90% diffusion burn duration. Although the overall burn duration was very similar between fuels, the diffusion burn rate between the 50% and 90% MFB locations was generally shorter for FT.
- Peak combustion pressures were very similar for each fuel type.
- FT NO_x brake specific emissions were lower than standard diesel fuel at all key states except for the medium-speed, medium-load condition at key state 8.
- PM emissions at the low-speed, medium-load condition were significantly lower for FT fuel.
- Carbon monoxide (CO) brake specific emissions were lower for FT fuel at all engine conditions except at key state 4 (medium speed, high load).
- Total hydrocarbon (THC) brake specific emissions were lower for FT fuel at all engine conditions.
- THC emissions are correlated to ignition delay and, hence, the effect of cetane number.
- It is likely that the significantly higher cetane number and lower density of the FT fuel were largely responsible for the observed differences in their combustion characteristics.

Publications: Two papers resulting from the FY01 effort were developed:

- McMillian, M.H., and Gautam, M. (2001). Combustion and emission characteristics of Fischer-Tropsch and standard diesel fuel in a single-cylinder diesel engine. SAE Paper 2001-01-3517.
- McMillian, M.H., Robey, E., and Gautam, M. (2002). Mutagenic potential of particulate matter from diesel engine operation on Fischer-Tropsch fuel as a function of engine operating conditions and particle size. Submitted to SAE International Spring Fuels and Lubricants Conference, Reno, NV, May 6- 8, 2002.

2.0 Natural Gas Engine Knock Abatement Studies

Description: Knock often occurs so rapidly and with such violence that the operator or engine controller cannot compensate fast enough to avoid engine damage. Damage due to knock is directly related to the rapid energy release in the combustion chamber due to autoignition. Continued engine operation under these conditions exacerbates autoignition and leads to eventual engine failure. Knock may be controlled by varying the fuel chemistry, through thermal management, or through novel mechanical design. Since fuel chemistry is often uncontrolled in stationary field applications, solutions must involve thermal, fluid mechanical, or mechanical methods. Increasing power density improves engine efficiency because the relative portion of useful power to frictional losses increases. Since most natural gas-fueled engines used in the power generation market use a spark-ignited, homogeneous-charge combustion system, the fundamental limit to an increase in power density is knock. Knock is a function of many engine variables, particularly bore size, compression ratio, air-fuel ratio, and inlet manifold temperature and pressure. Knock mitigation techniques generally reduce the rate of the knock pre-reactions in the air-fuel mixture and/or decrease the time for pre-reactions to occur. Thermal control may be accomplished by reducing the compression ratio or introducing exhaust gases (EGR), both of which act to lower flame speeds and decrease pre-reaction rates.

A rapid compression machine (RCM) approach has been chosen to circumvent the considerable cyclic variation in reciprocating engines and to provide ease of access and flexibility. The RCM design will allow easy changes to the geometry of the piston and head. This design flexibility is important, since pressure distribution and resultant fluid motion affect ignition delay time. Detonation waves can also be induced to positively interfere as a result of

geometric features. The RCM will employ temperature-controlled (heated and cooled) surfaces that may also aid in delineation of the effects of surface temperature distributions on knock. The RCM will employ flexibility for numerous spark sources by varying location, number, and type of spark (conventional or laser). We will work with generic geometric configurations designed to develop basic relationships and understanding of the effects of fluid dynamics, detonation phenomena, and knock.

There has been significant effort in the automotive industry addressing the issue of engine knock modeling. However, stationary natural gas engines have not fully utilized the results of these efforts. Currently available gas combustion kinetic mechanisms such as the GRI mechanism have excellent high temperature behavior. Low temperature reaction pathways need to be added for methane, ethane, propane, and, possibly, higher hydrocarbons to adequately predict knocking autoignition delay times and subsequent knocking behavior in fully coupled engine CFD models.

Fluent is presently working on an NETL-sponsored project to incorporate an ignition model into FLUENT for a fully-premixed natural gas-fueled system. This ignition model will use the full, detailed chemical mechanism of the GRI-MECH set of chemical reactions describing natural gas combustion. Turbulent flame propagation from the initial spark kernel will be modeled with a reaction progress model. Pressure waves originating from the flame front and the moving components of the RCM will be captured in the simulation. The pressure waves, and corresponding temperature fluctuations, will cause local auto-ignition. The perfectly premixed nature of the system enables the chemistry to be accurately parameterized by three variables, namely the pressure, temperature, and reaction progress. In turn, the expensive chemistry integration will be computed a-priori and tabulated, allowing rapid simulation of 3D moving mesh geometries with advanced turbulence models, including Reynolds Stress Models (RSM) and Large Eddy Simulation (LES). With the assumption of a perfectly premixed initial field, the model incorporates the relevant underlying physics and chemistry, and accurate simulations are anticipated.

Accomplishments: An initial literature review was completed in FY01. An initial model was established, and a model validation effort has begun. The experiments of Lee et al. were chosen for initial validation. These experiments consisted of a rapid compression machine working at various initial conditions. Nitrogen was used as a working fluid, as was a hydrogen/oxygen/argon mixture. These experiments were chosen for several reasons. Firstly, the nitrogen data allowed for a non-reacting check of Fluent's RCM set up. Secondly, the reacting data is for a simple fuel whose combustion is fairly well understood. Lastly, the piston crevice was redesigned to prevent piston roll-up, a problem which results in non-uniform core temperatures and frequently complicates RCM simulations.

The adiabatic compression pressure of nitrogen is shown in Figure 1 versus the simulated results of Lee et al. The peak pressure is matched well. There is some discrepancy during the compression process, which is likely due to differences in piston velocity and a variable crevice volume. The peak pressure remains constant after full compression. It was found that vortex rollup was predicted in the simulation, much as was found by Lee et al. For the non-adiabatic case, a different mesh was used which had a crevice volume equal to that reported in the literature (although the shape is not the same as the experiment). A boundary layer is used on all walls. The non-adiabatic compression pressure of nitrogen is shown in Figure 2 compared with the experimental data. The pressure decreases with time due to heat transfer, yet the peak pressure is over predicted. Possible explanations for this discrepancy that are being investigated include:

1) Crevice volume changes over time
2) Boundary layer needs more resolution (see temperature contours in Figure 3)
3) Crevice blow-by unaccounted for
4) Turbulence is enhancing the heat transfer
5) Crank angle dependency of specific heat ratio (k).

To validate the ignition chemistry such that it can be used with confidence, an adiabatic constant volume bomb was simulated. A detailed mechanism with 4 species and 25 reactions was used with a fractional step method of integrating the differential equations. All cases had an initial temperature of 1000 K and used H_2/O_2/Ar mixtures in 2/1/5 proportions (mole fraction). This is the same ratio as the RCM experiments that will be used. The initial pressure varied. This effort is continuing through FY02. Future work will focus on:

1) Improving pressure prediction
2) Simulating reacting H2/O2/Argon RCM
3) Simulating methane/air RCM data from NETL RCM

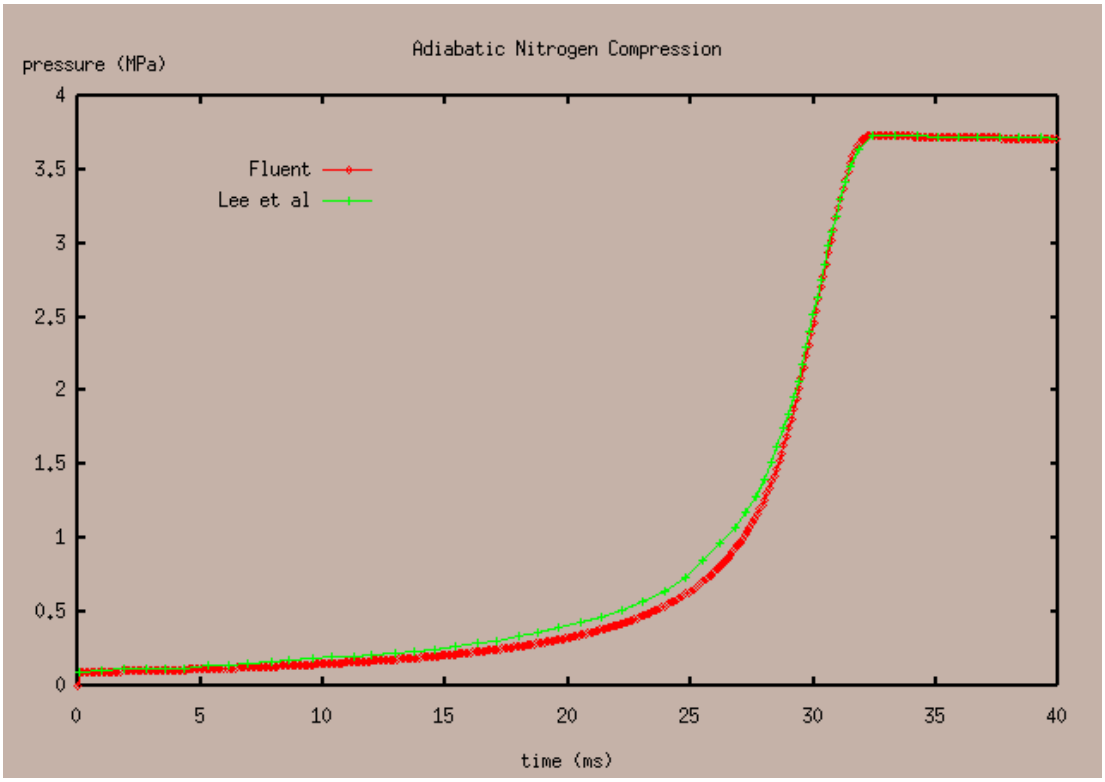

Figure 1: Pressure versus time for the adiabatic nitrogen compression case.

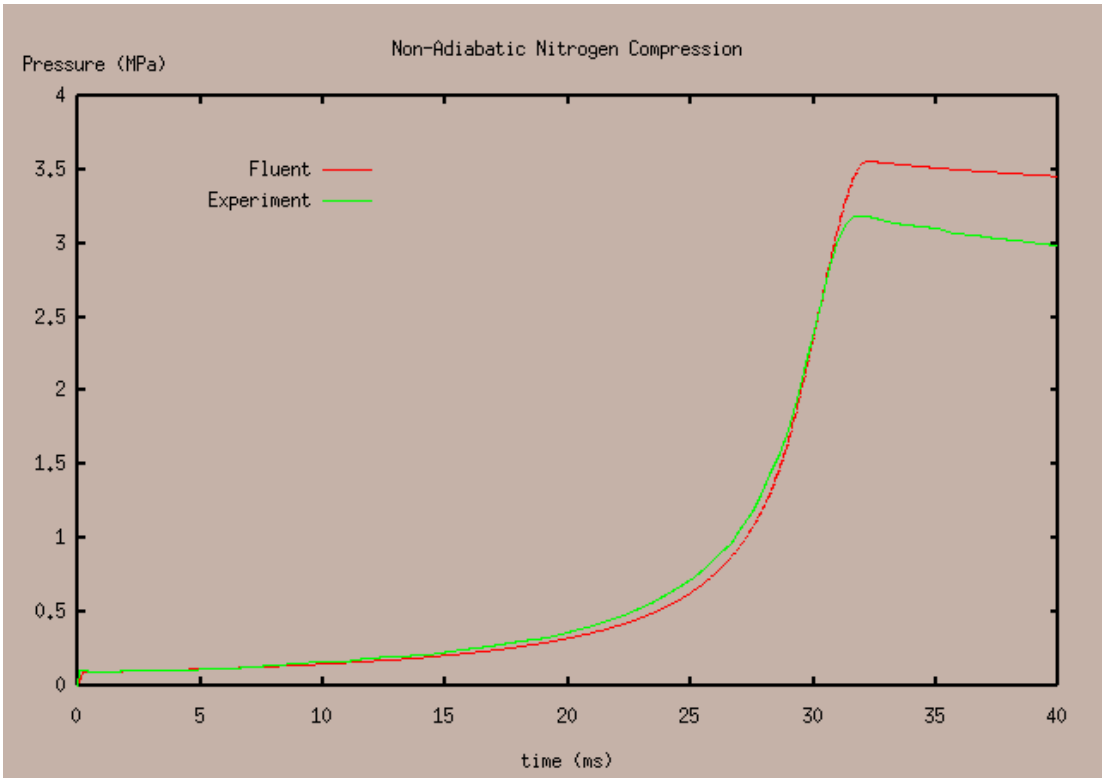

Figure 2: Pressure versus time for non-adiabatic nitrogen compression (no crevice model used).

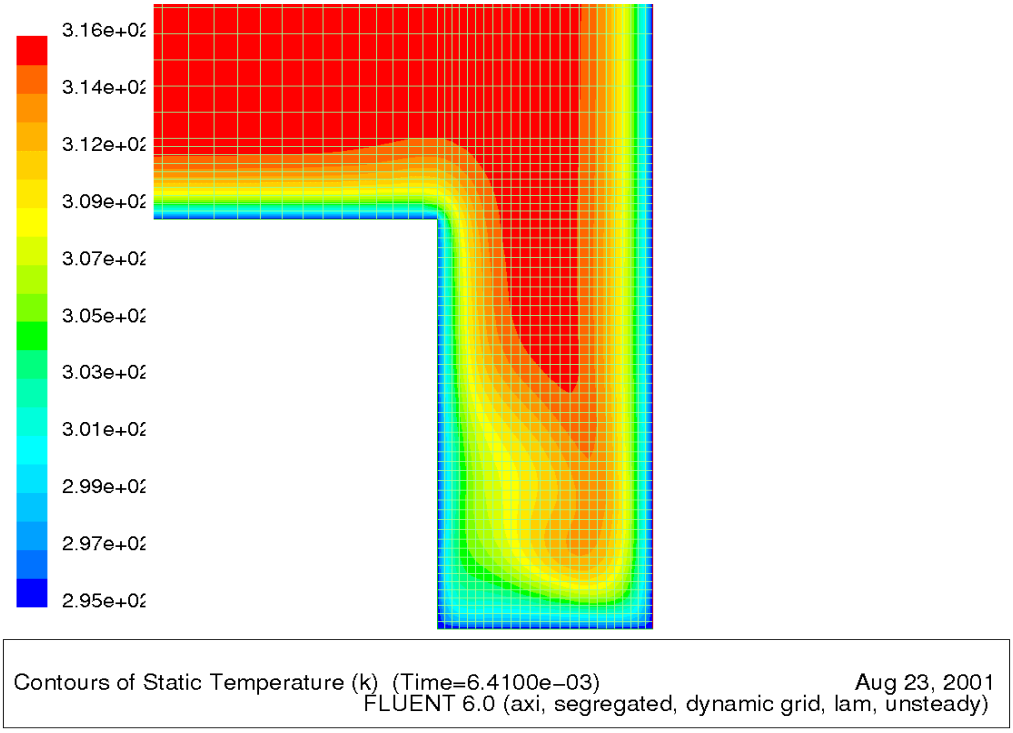

Figure 3: Temperature contours in crevice for non-adiabatic nitrogen compression.

Publications:

- Yavuz, I., Celik, I., and McMillian, M.H. (2002). Knock prediction in reciprocating gas-engines using detailed chemical kinetics. SAE Paper No. 2001-01-1012.

3.0 Infrared Diode Laser Ignition System for Ultra-Lean Natural Gas Engines

Description: Natural gas is an attractive alternative fuel for reciprocating engines because of the potential for meeting the increasing demands in the areas of thermal efficiencies and power densities, reduced fuel costs, and reduced particulate emissions. To obtain these goals, fuel-lean operation is more desirable because the thermodynamic properties of the mixture are closer to ideal. By operating fuel-lean the efficiency and specific fuel consumption of the engines can be increased, while reducing NO_x and other toxic gases emissions. This is because fuel-lean combustion yields lower operating temperatures resulting in lower NO_x and lower heat losses. Further, a higher compression ratio can be used with leaner mixtures. However, lean operation leads to slow initial flame kernel development, in turn leading to lower burning velocity and longer ignition time. Lean operation also leads to an increase in cyclic variability, which results in some cycles either not burning completely (partial burn limit) or not igniting at all (misfire limit).

The use of a laser as an ignition source has many potential benefits, including greater control over the timing and location of ignition. Laser radiation can be positioned at a considerable distance from the point of ignition, thus eliminating distortions due to wall effects and problems involving heat loss through electrodes such as misfire. Laser ignition provides multiple ignition sites at varying times and locations under closed-loop control. This would enable one to avoid some of the problems associated with lean-fuel combustion. In addition, if a flame is initiated simultaneously at many points throughout the mixture volume, the total burning time could be much smaller than using a single-site ignitor.

Accomplishments:

1. Laser Spark Ignition of a Jet Diffusion Flame

For this task, the laser ignition probability of a methane diffusion jet flame was studied in order to demonstrate the effectiveness of laser ignition in a turbulent environment. The gas jet was produced using a contoured stainless steel nozzle with an inlet diameter of 2.5 cm and a flat exit tip diameter of 0.15 cm. The nozzle was mounted on a three-axis translation stage and was aimed vertically upward into the laboratory air. Research grade methane (99.99%) was used. Sparks were produced using a single-mode, Q-switched Nd-YAG laser. The laser produced a 0.6-cm-diameter beam at a wavelength of 1064 nm with a 5.5 ns pulse duration. To preserve the quality of the laser beam throughout the experiments, the focal point was kept at a fixed location, and the relative location of the laser spark along the jet axis was varied by translating the gas nozzle vertically. Once a vertical location was chosen, the nozzle could be translated horizontally in a direction perpendicular to both the jet axis and the laser beam. The combined motions permit a complete radial and axial scan of the jet region. The location of the optimum ignition probability varies with the flow conditions. Off-jet axis and near-nozzle ignition locations lead to longer blow out times. The distribution of the ignition probability can be attributed to the variations in the fuel-to-air ratio at various locations within the jet. Other factors such as turbulence intensity and velocity gradient at the ignition location also influence the ignition probability. It is known that when a fuel jet enters quiescent air, jet expansion and air entrainment occur. These results illustrate the benefits of laser ignition for ignition and flame stabilization applications because of the ease of moving the ignition site.

2. An Experimental study of the laser-induced spark evolution and ignition

The objective of this effort was to optically characterize the physical and chemical processes underlying the evolution of and the interaction between the spark and the combustible ambient gas leading to ignition. The

evolution of the laser spark was detected using the beam deflection technique. The deflected HeNe beam is detected by a fast receiver unit, a fiber optic cable (200 μm core diameter), and a narrow band interference filter centered at 632.8 nm. The receiver unit was located approximately 3 m from the region of interest. The time-resolved OH emissions were measured using a fast PMT (2 ns rise time), a 12-nm wide interference filter centered at 308 nm, and imaging optics. The PMT and the imaging optics were set up to view the ignition location having a diameter of about 5 mm. It is known that when a laser spark is created, it expands supersonically into the ambient gas in all directions. As the shock wave propagates, it heats and ionizes the gas on its path, leading to an increase in the spark plasma volume. Thus, the evolution of the laser spark consists of many consecutive phases and processes starting with the onset of the spark, the formation and the propagation of the shock wave front, and the expansion of the spark volume. It is followed by shock detachment and after-shock perturbation as typically shown in Fig. 4. The whole process of spark evolution lasts only on the order of a microsecond or less, which is short (by 2 orders of magnitude) compared to the observed ignition times (milliseconds). Thus, although the shock expansion and the late-time perturbation may be important in the mixing of active reagents created by the early shock, the expanding shock could not directly ignite the ambient combustible gas. It is hypothesized that, after expansion, the spark leaves behind a volume of very high temperature and low-density gas. The hot ball of gas then interacts with the surrounding gas, leading to ignition. This ignition mechanism is supported by data on the OH emission shown in Fig. 5. There are two time periods within which the OH emission was clearly detected: the early-time OH emission and the late-time OH emission. In between, however, the OH emission was too weak to be detectable. The early-time OH emission was due to the chemical reactions associated with the decay of the breakdown spark and the evolution of the shock. It appeared almost immediately after formation of the spark (from a few hundred nanoseconds to microseconds) and then disappeared after the shock expansion had stopped (about 150 μs later). The late-time OH emission was detected at about 1.5 ms after the shock expansion had ceased; its intensity continued to increase leading to ignition and full combustion. It is obvious that the late-time OH emission is due to the chemical reactions that are induced by the hot ball of gas remaining after the shock expansion. It is also important to report that early-time OH emission was always observed in the present experiments, but not all these sparks yielded successful ignition. Successful ignition, however, is always associated with a strong OH emission at later times. Thus, chemical reactions during the initial stage of the blast wave expansion are not responsible for the ignition. Rather, the ultimate fate of an ignition depends on the reactions in the later time, which determines whether the gas could undergo a transition from hot plasma to a

propagating flame.

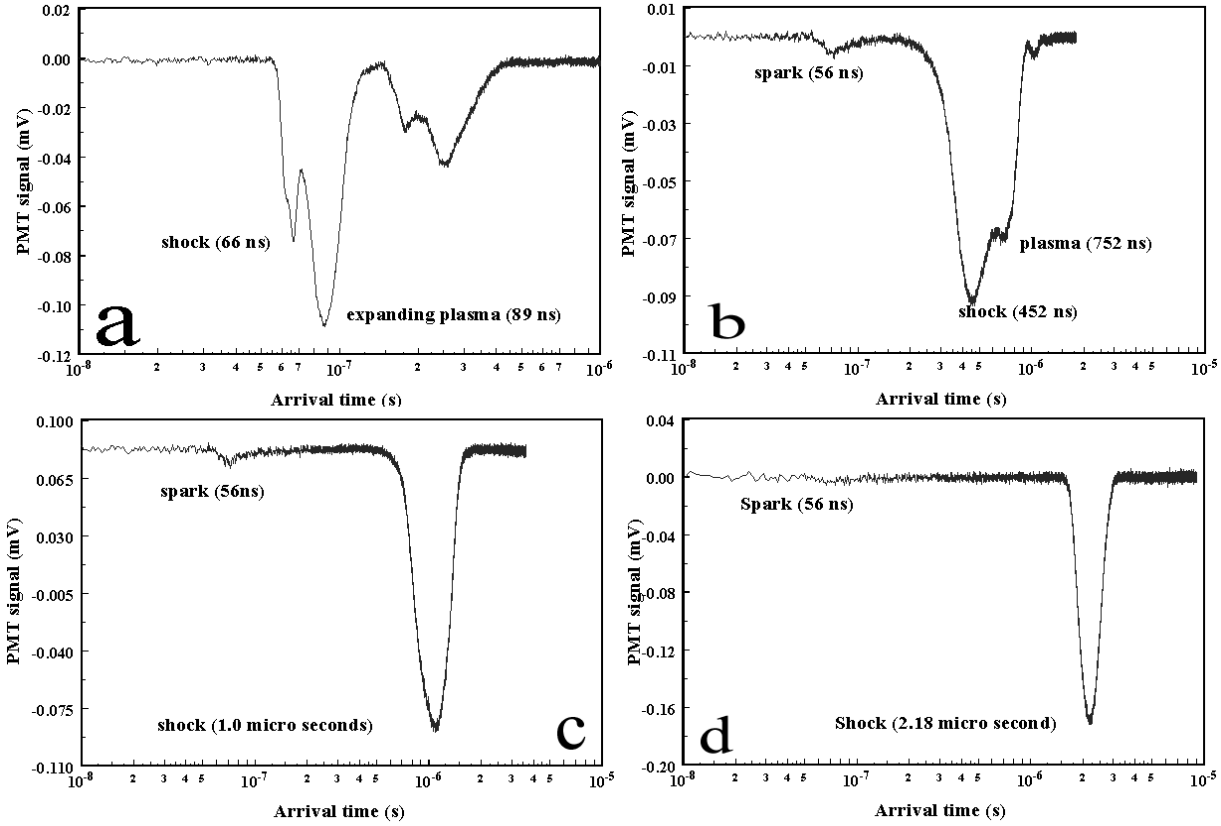

Figure 4. Evolution of the laser-induced spark shock wave 30 mJ; (a: laser beam was 0.4 mm, b: 0.8 mm, c: 1.2 mm, and d: 1.6 mm above the spark).

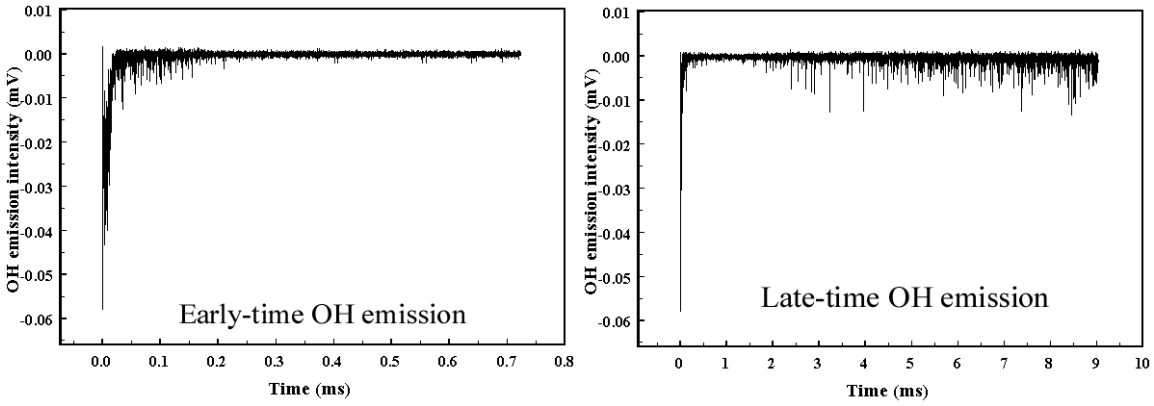

Figure 5. Time-resolved OH emission from an ignition event

3. Laser-Induced Spark for Measurements of the Fuel-to-Air Ratio

This task is aimed at the use of the laser-induced spark for simultaneous measurements of the ignition and fuel-to-air ratio of a combustible mixture. The relative amounts of fuel and air concentrations at the laser focus have been estimated using a variant of laser-induced breakdown spectroscopy. In essence, we examine the late time behavior of the line radiation at the wavelength of the OI triplet near 777 nm and at the wavelength of the H_α

line, 656 nm, which is emitted by electronically excited hydrogen dissociated from the methane fuel. The results are shown in Figs. 6 and 7. Figure 6 shows that when a fuel jet enters quiescent air, jet expansion and air entrainment occur. Entrained air mixes with the fuel to form a flammable mixture in the flow field. Since the mixing rate in this case depends on the turbulent interaction between the jet and the entrained air (which depends strongly on the jet velocity), the fuel and air concentrations across the jet and along its axis are different. In the region near the nozzle tip, entrained air does not have time to penetrate and mix with the fuel, so the fuel concentration across the jet might be too rich to ignite. Above the nozzle tip, since the air has sufficient time to penetrate into the jet, there is a region where the fuel concentration decreases from rich, to stoichiometric, to lean on moving radially toward the air side. As the latter site is further away from the nozzle tip, there is a flammable region where a stoichiometric fuel fraction exists across the jet. At the top of the jet, however, the flow field may become too lean to burn. Figure 7 shows the ignition probability and equivalence ratio in the radial locations for

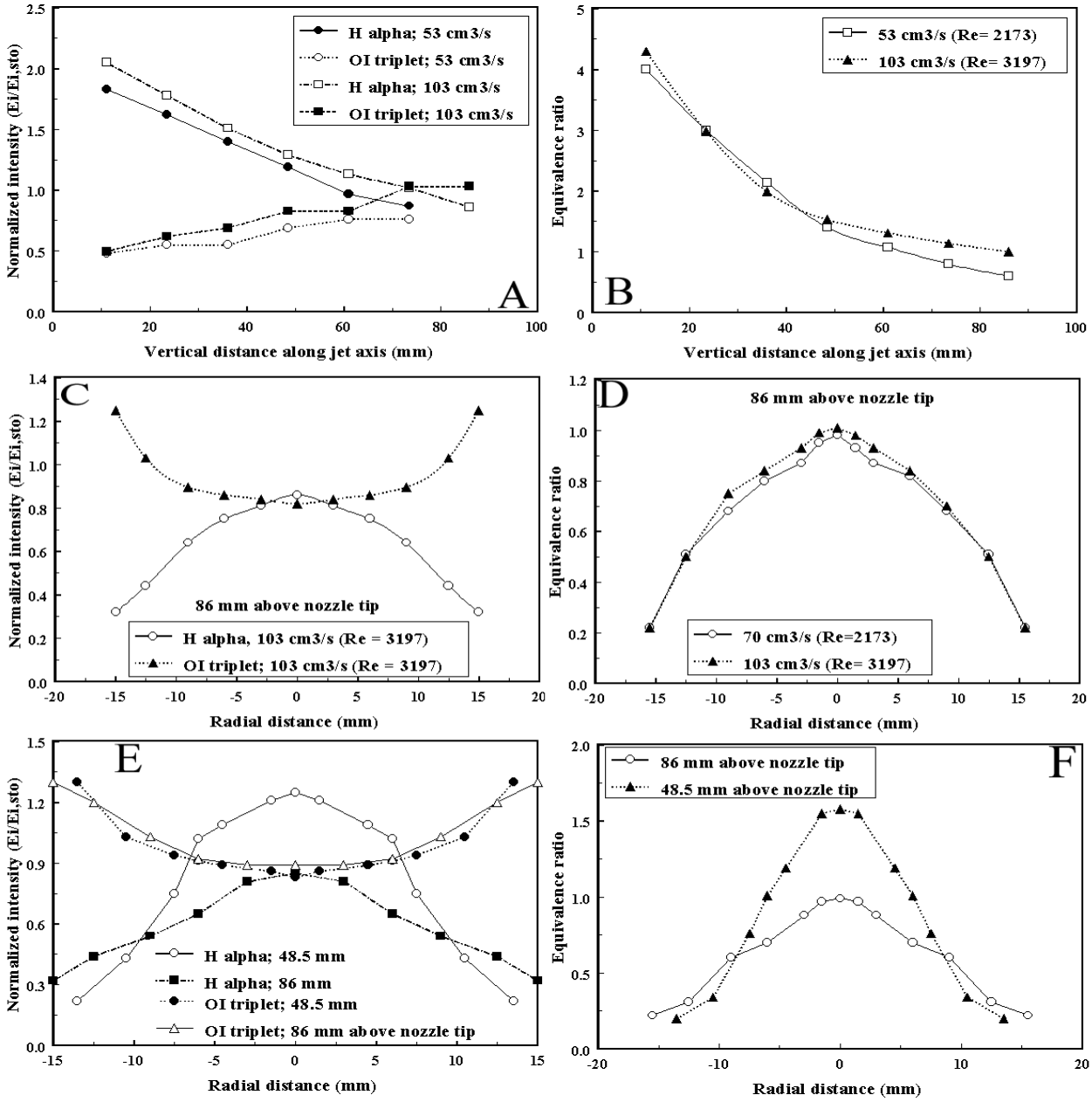

the jet flow rate of 70 cm^3/s (Re=2173) at 48.5 mm above the nozzle tip.

Figure 6. Normalized emission intensities of H_α line (656nm) and OI triplet (777nm) and equivalence ratio of a methane jet diffusion flame. ($H_{\alpha,sto}$=185 mV; OI = 14.5 mV); (A & B: in the vertical along the jet axis; C&D: in the radial direction at 86 mm above the nozzle tip; E&F: in the radial direction; effect of the vertical locations (70 cm^3/; Re = 2173))

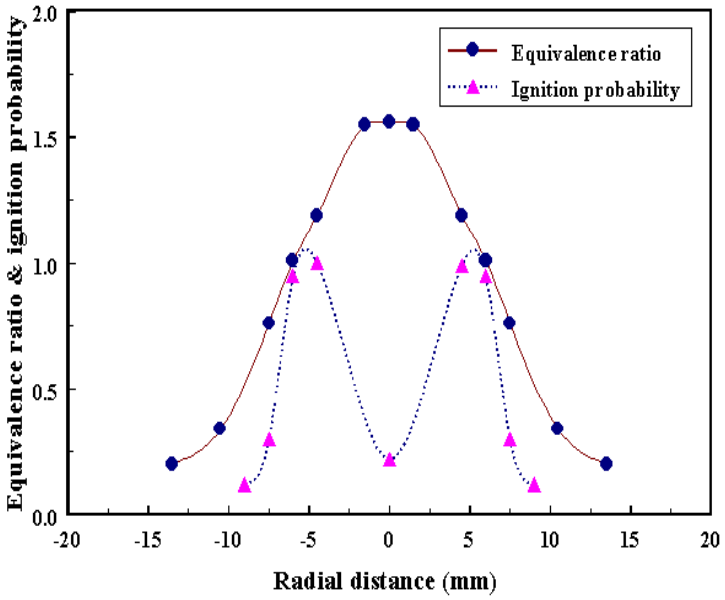

Figure 7. Ignition probability and equivalence ratio in the radial locations for the jet flow rate of 70 cm^3/s (Re=2173) at 48.5 mm above the nozzle tip.

4. AN OPTICAL AND SPECTROSCOPIC STUDY OF THE LASER-INDUCED SPARK FOR DETERMINATION OF THE LASER MINIMUM IGNITION ENERGY

Laser spark minimum ignition energies reported thus far show several features. The laser ignition energy depends on the focal spot volume and pressure. Longer focal length lens and lower pressure tend to require higher ignition spark energy. The effect of the pressure is due to the decreased collisional frequency and number density of the fuel molecules in the ignition volume, and hence higher energy is required. For hydrocarbon ignition, in order to have sufficient fuel for the ignition kernel to grow, a fuel-rich condition is necessary. This is due to the rapid depletion of the fuel at the ignition point and the relatively slow diffusion of the fuel toward the ignition point. Generally, the ignition energies are similar to the minimum ignition energies measured using electric spark in the far-lean and far-rich regions. However, in the stoichiometric or near-stoichiometric region, the laser ignition energy is consistently higher than the minimum ignition energy using electric spark ignition.

The reason that the laser ignition requires higher ignition energy is due to the fact that a large portion of the absorbed energy is used up, in the forms of blast-wave losses and radiation/convection losses, within the first microsecond or less. The actual energy that is available for causing ignition is that of the hot gas that is left behind after the shock front has propagated away. Thermal radiation losses are also important, which can account for a significant fraction of the absorbed energy in the early stage of the plasma expansion, even in the case where the convection losses are large. The thermal radiation consists of mechanisms that are atomic in nature. Generally, it consists of several continuum radiation spectra due to plasma recombination of free-bound transition, free-free transition (bremsstrahlung), negative ion emission, spectral line radiation, and pseudo-continuum of strongly broadened lines. The free-free radiation is due to the interaction of a free electron with the electric field of an ion. In this process the kinetic energy of the electron is reduced by the energy of the emitted photon. The recombination is the process by which an electron is captured by an ion of charge (z-1)e. We have quantified these energy losses. For the range of spark energies from 15 to 50 mJ, the shock front reached the sonic radius of about 2.3 to 3.6 mm within a microsecond or less. During this period the shock-wave energy loss was about 51% to 70%, the radiation energy losses accounted for 22% to 34%, and the energy of the remaining hot gas, which provides the energy for ignition, was about 7% to 8% of the absorbed energy. For example, within the ranges of the ignition energies reported for a stoichiometric methane-air mixture, the actual ignition energies would be around 0.36 to 0.4 mJ, the values that are consistent with those provided by electrical spark ignition. Thus, to within the limits of error of the present measurements and calculations, the ignition energy required for laser spark ignition will not differ greatly from that required for electric spark ignition.